Progress In Electromagnetics Research M, Vol. 68, 181–191, 2018

Average Intensity of Partially Coherent Lorentz Beams in Oceanic Turbulence

Dajun Liu* and Yaochuan Wang

Abstract—Partially coherent Lorentz beams have been introduced to describe the output of the diode laser, which have been investigated due to the special spreading properties. The analytical expressions of partially coherent Lorentz beam propagating in oceanic turbulence are derived. Using the derived equations, the average intensity distributions of partially coherent Lorentz beam are analyzed and discussed. It is shown that the partially coherent Lorentz beam with smaller coherence length will evolve into the Gaussian-like beam faster, and the beam propagation in oceanic turbulence will spread faster with increasing strength of oceanic turbulence. The results have potential application in underwater optical communications and sensing.

1. INTRODUCTION

Recently, many new types of laser beams have been introduced to describe the output of diode laser. Among them, Lorentz beam has been provided to describe the light field of diode laser [1]. Since the model of Lorentz beams is introduced, the propagation properties of Lorentz and Lorentz-like beams have been investigated by many scientists. In the past years, the properties of Lorentz and partially coherent Lorentz beams propagating in uniaxial crystal have been illustrated and analyzed [2–5]. The partially coherent Lorentz-Gauss beam propagating through ABCD optical system has been investigated [6]. In the field of beam propagation in random media, the evolution properties of Lorentz-like beam in random media have been widely investigated [7–14]. In the studies of nonparaxial propagation, the nonparaxial propagation properties and far-field propagation properties of Lorentz-like beam have also been widely studied [15–17].

With the application of laser technology in underwater, the evolution properties of laser beams propagating in oceanic turbulence have been investigated. In recent years, the propagation properties of various laser beams in oceanic turbulence have been illustrated and analyzed, including the scintillation index of laser beam [18], mutual coherence function of laser beam [19], astigmatic stochastic electromagnetic beam [20], partially coherent flat-topped vortex hollow beam [21], partially coherent annular beam [22], Gaussian Schell-model vortex beam [23], stochastic electromagnetic vortex beam [24], flat-topped vortex hollow beam [25], partially coherent Hermite-Gaussian linear array beam [26], partially coherent four-petal Gaussian vortex beam [27], Gaussian array beam [28–30], partially coherent cylindrical vector beam [31], chirped Gaussian pulsed beam [32], Lorentz beam [33] and partially coherent four-petal Gaussian beam [34]. To the best of our knowledge, there has been no report on the propagation analysis of partially coherent Lorentz beams propagating in oceanic turbulence. In this paper, based on the derived equations, the average intensity of beams propagating in oceanic turbulence has been analyzed, and influences of oceanic turbulence have been given.

Received 20 March 2018, Accepted 10 May 2018, Scheduled 25 May 2018
* Corresponding author: Dajun Liu (liudajun@dlmu.edu.cn).
The authors are with the Department of Physics, College of Science, Dalian Maritime University, Dalian 116026, China.

2. PROPAGATION OF PARTIALLY COHERENT LORENTZ BEAMS IN OCEANIC TURBULENCE

In the Cartesian coordinate system, the cross-spectral density function of partially coherent Lorentz beams generated by Schell-model source propagating along the z axis at the source plane $z = 0$ can be expressed as [11]:

$$\begin{aligned} W\left(\mathbf{r}_{10}, \mathbf{r}_{20}, 0\right) = & \frac{1}{w_{0x}^2 w_{0y}^2\left[1+\left(\frac{x_{10}}{w_{0x}}\right)^2\right]\left[1+\left(\frac{y_{10}}{w_{0y}}\right)^2\right]} \frac{1}{\left[1+\left(\frac{x_{20}}{w_{0x}}\right)^2\right]\left[1+\left(\frac{y_{20}}{w_{0y}}\right)^2\right]} \\ & \times \exp\left[-\frac{\left(x_{10}-x_{20}\right)^2}{2\sigma_x^2}-\frac{\left(y_{10}-y_{20}\right)^2}{2\sigma_y^2}\right] \end{aligned} \tag{1}$$

where $\mathbf{r}_{10} = (x_{10}, y_{10})$ and $\mathbf{r}_{20} = (x_{20}, y_{20})$ are the position vectors at the plane $z = 0$; w_{0x} and w_{0y} are the beam width radius of the beam in the x and y directions, respectively. σ_x and σ_y are the coherence length.

Based on the previous reports, the Lorentz distribution in Equation (1) can be written as [35]

$$\begin{aligned} \frac{1}{\left(x_0^2+w_{0x}^2\right)\left(y_0^2+w_{0y}^2\right)} = & \frac{\pi}{2w_{0x}^2 w_{0y}^2}\sum_{m=0}^{N}\sum_{n=0}^{N} a_{2m}a_{2n}H_{2m}\left(\frac{x_0}{w_{0x}}\right)H_{2n}\left(\frac{y_0}{w_{0y}}\right) \\ & \times \exp\left(-\frac{x_0^2}{2w_{0x}^2}-\frac{y_0^2}{2w_{0y}^2}\right) \end{aligned} \tag{2}$$

where N is the term number of the expansion; a_{2m} and a_{2n} are the expanded coefficients given in [35]. As the even number $2m$ and $2n$ increase, the value of expanded coefficients a_{2m} and a_{2n} will decrease dramatically. Therefore, N will not be too large in the numerical calculations. In this work, N is chosen as $N = 5$. The Hermite polynomial $H_{2m}(x)$ in Equation (2) can be expressed as [36]:

$$H_{2m}(x) = \sum_{l=0}^{m} \frac{(-1)^l (2m)!}{l!(2m-2l)!}(2x)^{2m-2l} \tag{3}$$

By submitting Equation (2) in Equation (1), the cross-spectral density function of partially coherent Lorentz beams at the source plane $z = 0$ can be rewritten as:

$$\begin{aligned} W\left(\mathbf{r}_{10}, \mathbf{r}_{20}, 0\right) = & \frac{\pi^2}{4w_{0x}^2 w_{0y}^2}\sum_{m=0}^{N}\sum_{n=0}^{N}\sum_{m'=0}^{N}\sum_{n'=0}^{N} a_{2m}a_{2n}a_{2m'}a_{2n'} \\ & \times H_{2m}\left(\frac{x_{10}}{w_{0x}}\right)H_{2n}\left(\frac{y_{10}}{w_{0y}}\right)H_{2m'}\left(\frac{x_{20}}{w_{0x}}\right)H_{2n'}\left(\frac{y_{20}}{w_{0y}}\right) \\ & \times \exp\left(-\frac{x_{10}^2}{2w_{0x}^2}-\frac{y_{10}^2}{2w_{0y}^2}\right)\exp\left(-\frac{x_{20}^2}{2w_{0x}^2}-\frac{y_{20}^2}{2w_{0y}^2}\right) \\ & \times \exp\left[-\frac{\left(x_{10}-x_{20}\right)^2}{2\sigma_x^2}-\frac{\left(y_{10}-y_{20}\right)^2}{2\sigma_y^2}\right] \end{aligned} \tag{4}$$

Based on the extended Huygens-Fresnel principle, the cross-spectral density function of partially coherent beams propagating in oceanic turbulence can be expressed as [20–22]:

$$\begin{aligned} W\left(\mathbf{r}_1, \mathbf{r}_2, z\right) = & \frac{k^2}{4\pi^2 z^2}\int_{-\infty}^{+\infty}\int_{-\infty}^{+\infty}\int_{-\infty}^{+\infty}\int_{-\infty}^{+\infty} W\left(\mathbf{r}_{10}, \mathbf{r}_{20}, 0\right)\times\exp\left[-\frac{ik}{2z}\left(\mathbf{r}_1-\mathbf{r}_{10}\right)^2+\frac{ik}{2z}\left(\mathbf{r}_2-\mathbf{r}_{20}\right)^2\right] \\ & \times\left\langle\exp\left[\psi\left(\mathbf{r}_{10}, \mathbf{r}_1\right)+\psi^*\left(\mathbf{r}_{20}, \mathbf{r}_2\right)\right]\right\rangle d\mathbf{r}_{10}d\mathbf{r}_{20} \end{aligned} \tag{5}$$

where $W(\mathbf{r}_1, \mathbf{r}_2, z)$ is the cross-spectral density function of partially coherent beam at the receiver plane z; $\mathbf{r} = (x, y)$ is the position vector at the receiver plane z; λ is the wavelength, and $k = 2\pi/\lambda$ is the wave number; $\psi(\mathbf{r}_0, \mathbf{r}, z)$ is the solution to the Rytov method that represents the random part of the complex phase for the oceanic turbulence. The asterisk denotes the complex conjugation. The last term in Equation (6) can be written as:

$$\langle \exp\left[\psi\left(\mathbf{r}, \mathbf{r}_{10}\right) + \psi^*\left(\mathbf{r}, \mathbf{r}_{20}\right)\right]\rangle = \exp\left\{-M\left[\left(\mathbf{r}_{10} - \mathbf{r}_{20}\right)^2 + \left(\mathbf{r}_{10} - \mathbf{r}_{20}\right)\left(\mathbf{r}_1 - \mathbf{r}_2\right) + \left(\mathbf{r}_1 - \mathbf{r}_2\right)^2\right]\right\} \tag{6}$$

with

$$M = \frac{\pi^2 k^2 z}{3} \int_0^\infty d\kappa \kappa \Phi(\kappa) \tag{7}$$

The spatial power spectrum of the oceanic turbulence $\Phi(\kappa)$ can be expressed as

$$\begin{aligned} \Phi(\kappa) \; = \; & 0.388 \times 10^{-8} \varepsilon^{-11/3} \left[1 + 2.35 \left(\kappa\eta\right)^{2/3}\right] f\left(\kappa, \varsigma, \chi_T\right) \\ & \times \frac{\chi_T}{\varsigma^2} \left[\varsigma^2 \exp\left(-A_T \delta\right) + \exp\left(-A_S \delta\right) - 2\varsigma \exp\left(-A_{TS} \delta\right)\right] \end{aligned} \tag{8}$$

where ε is the rate of dissipation of dissipation of turbulent kinetic energy per unit mass of fluid, which may vary in the rage from $10^{-1}\,\mathrm{m^2s^{-3}}$ to $10^{-10}\,\mathrm{m^2s^{-3}}$; $\eta = 10^{-3}$ is the Kolmogorov micro (inner scale); χ_T is the rate of dissipation of mean square temperature taking value in the range from $10^{-4}\,\mathrm{K^2s^{-1}}$ to $10^{-10}\,\mathrm{K^2s^{-1}}$, $A_T = 1.863 \times 10^{-2}$, $A_S = 1.9 \times 10^{-4}$, $A_{TS} = 9.41 \times 10^{-3}$, $\delta = 8.284(\kappa\eta)^{4/3} + 12.978(\kappa\eta)^2$; ς is the relative strength of temperature and salinity fluctuations, which can vary in the rage from -5 to 0.

Substituting Equation (3) into Equation (5) and recalling the following equations [36]:

$$\int_{-\infty}^{+\infty} H_{2m}(x) \exp\left[-a\left(x-y\right)^2\right] dx \; = \; \sqrt{\frac{\pi}{a}}\left(1 - \frac{1}{a}\right)^m H_{2m}\left[y\left(1 - \frac{1}{a}\right)^{-1/2}\right] \tag{9}$$

$$\int_{-\infty}^{+\infty} x^n \exp\left(-px^2 + 2qx\right) dx \; = \; n! \exp\left(\frac{q^2}{p}\right)\left(\frac{q}{p}\right)^n \sqrt{\frac{\pi}{p}} \sum_{k=0}^{\left[\frac{n}{2}\right]} \frac{1}{k!\,(n-2k)!}\left(\frac{p}{4q^2}\right)^k \tag{10}$$

We can obtain

$$\begin{aligned} W\left(\mathbf{r}_1, \mathbf{r}_2, z\right) \; = \; & \frac{k^2}{4\pi^2 z^2}\left(\frac{\pi}{2w_{0x}w_{0y}}\right)^2 \exp\left[-\frac{ik}{2z}\mathbf{r}_1 + \frac{ik}{2z}\mathbf{r}_2\right] \\ & \times \exp\left[-M\left(x_1 - x_2\right)^2 - M\left(y_1 - y_2\right)^2\right] \times W\left(x, z\right) W\left(y, z\right) \end{aligned} \tag{11}$$

with

$$\begin{aligned} W\left(x, z\right) \; = \; & \sum_{m=0}^{N} \sum_{m'=0}^{N} a_{2m} a_{2m'} w_{0x} \sqrt{\frac{\pi}{a_x}}\left(1 - \frac{1}{a_x}\right)^m \exp\left\{\frac{w_{0x}^2}{4a_x}\left[2\frac{ik}{2z}x_1 - M\left(x_1 - x_2\right)\right]^2\right\} \\ & \times \sum_{d=0}^{m} \frac{(-1)^d\,(2m)!}{d!\,(2m-2d)} \sum_{l=0}^{m'} \frac{(-1)^l\,(2m')!}{l!\,(2m'-2l)!}\left(\frac{2}{w_{0x}}\right)^{2m'-2l}\left[\left(1 - \frac{1}{a_x}\right)^{-\frac{1}{2}} \frac{w_{0x}}{a_x}\right]^{2m-2d} \\ & \times \sum_{s=0}^{2m-2d} \frac{(2m-2d)!}{s!\,(2m-2d-s)!}\left[2\frac{ik}{2z}x_1 - M\left(x_1 - x_2\right)\right]^{2m-2d-s}\left[2\left(\frac{1}{2\sigma_x^2} + M\right)\right]^s \\ & \times \sqrt{\frac{\pi}{b_x}} 2^{-2m'+2l-s} i^{2m'-2l+s}\left(\frac{1}{\sqrt{b_x}}\right)^{2m'-2l+s} \exp\left(\frac{c_x^2}{b_x}\right) H_{2m'-2l+s}\left(-\frac{ic_x}{\sqrt{b_x}}\right) \end{aligned} \tag{12}$$

where

$$a_x \; = \; \left(\frac{1}{2w_{0x}^2} + \frac{1}{2\sigma_x^2} + M + \frac{ik}{2z}\right) w_{0x}^2 \tag{13a}$$

$$b_x = \frac{1}{2w_{0x}^2} + \frac{1}{2\sigma_x^2} + M - \frac{ik}{2z} - \frac{w_{0x}^2}{a_x}\left(\frac{1}{2\sigma_x^2} + M\right)^2 \tag{13b}$$

$$c_x = \frac{w_{0x}^2}{2a_x}\left[2\frac{ik}{2z}x_1 - M\left(x_1 - x_2\right)\right]\left(\frac{1}{2\sigma_x^2} + M\right) - \frac{ik}{2z}x_2 + \frac{M}{2}\left(x_1 - x_2\right) \tag{13c}$$

and

$$\begin{aligned} W\left(y, z\right) = & \sum_{n=0}^{N}\sum_{n'=0}^{N} a_{2n}a_{2n'}w_{0x}\sqrt{\frac{\pi}{a_y}}\left(1 - \frac{1}{a_y}\right)^n \exp\left\{\frac{w_{0y}^2}{4a_y}\left[2\frac{ik}{2z}y_1 - M\left(y_1 - y_2\right)\right]^2\right\} \\ & \times \sum_{d'=0}^{n}\frac{(-1)^{d'}(2n)!}{d'!\,(2n - 2d')!}\sum_{l'=0}^{n'}\frac{(-1)^{l'}(2n')!}{l'!\,(2n' - 2l')!}\left(\frac{2}{w_{0y}}\right)^{2m' - 2l'}\left[\left(1 - \frac{1}{a_y}\right)^{-\frac{1}{2}}\frac{w_{0y}}{a_y}\right]^{2n - 2d'} \\ & \times \sum_{s'=0}^{2n-2d'}\frac{(2n - 2d')!}{s'!\,(2n - 2d' - s')!}\left[2\frac{ik}{2z}y_1 - M\left(y_1 - y_2\right)\right]^{2n - 2d' - s'}\left[2\left(\frac{1}{2\sigma_y^2} + M\right)\right]^{s'} \\ & \times \sqrt{\frac{\pi}{b_y}}2^{-2n' + 2l' - s'}i^{2n' - 2l' + s'}\left(\frac{1}{\sqrt{b_x}}\right)^{2n' - 2l' + s'}\exp\left(\frac{c_y^2}{b_y}\right)H_{2n' - 2l' + s'}\left(-\frac{ic_y}{\sqrt{b_y}}\right) \end{aligned} \tag{14}$$

where

$$a_y = \left(\frac{1}{2w_{0y}^2} + \frac{1}{2\sigma_y^2} + M + \frac{ik}{2z}\right)w_{0y}^2 \tag{15a}$$

$$b_y = \frac{1}{2w_{0y}^2} + \frac{1}{2\sigma_y^2} + M - \frac{ik}{2z} - \frac{w_{0y}^2}{a_y}\left(\frac{1}{2\sigma_y^2} + M\right)^2 \tag{15b}$$

$$c_y = \frac{w_{0y}^2}{2a_y}\left[2\frac{ik}{2z}y_1 - M\left(y_1 - y_2\right)\right]\left(\frac{1}{2\sigma_y^2} + M\right) - \frac{ik}{2z}y_2 + \frac{M}{2}\left(y_1 - y_2\right) \tag{15c}$$

When $\mathbf{r}_1 = \mathbf{r}_2$ in Equations (11)–(15), the analytical expressions of partially coherent Lorentz beams propagating in oceanic turbulence can be obtained, by using the derived equations, and the average intensity of partially coherent Lorentz beams propagating in oceanic turbulence can be calculated and analyzed.

3. NUMERICAL EXAMPLES AND ANALYSIS

In this section, based on the derived equations in the above section, the average intensity of the partially coherent Lorentz beams propagating in oceanic turbulence are calculated and analyzed using numerical examples. In the following numerical calculations, the parameters are set as $\lambda = 417\,\mathrm{nm}$, $\lambda = 417\,\mathrm{nm}$, $w_{0x} = 2\,\mathrm{mm}$, $\sigma_x = \sigma_y = \sigma = 2\,\mathrm{mm}$, $\varsigma = -2.5$, $\chi_T = 10^{-8}\,\mathrm{K}^2/\mathrm{s}$, and $\varepsilon = 10^{-7}\,\mathrm{m}^2\mathrm{s}^{-1}$ in the whole paper.

First, the normalized average intensity of partially coherent Lorentz beams propagating in oceanic turbulence are studied. The normalized average intensities of partially coherent Lorentz beam for the different beam widths $w_{0y} = 2\,\mathrm{mm}$ and $w_{0y} = 4\,\mathrm{mm}$ are shown in Figures 1 and 2, respectively. One finds that the partially coherent Lorentz beams propagating in oceanic turbulence will spread as the propagation distance z increases, and the beam can keep its initial beam spot with the Lorentz distribution at the short propagation distance. The circular partially coherent Lorentz beam will keep its circular beam spot (Figure 1(a)), and the elliptical partially coherent Lorentz beam will keep its elliptical beam spot (Figure 2(b)). When the propagation distance z increases to the far field, the circular and elliptical partially coherent Lorentz beams will evolve into circular Gaussian beam. In order to investigate the influence of beam widths on evolution properties, the cross sections ($y = 0$) of partially coherent Lorentz beams propagating in oceanic turbulence for the different beam widths $w_{0y} = w_{0y} = w$ are illustrated in Figure 3. From Figure 3(a), it is found that the beam with larger beam width has larger beam spot at short propagation distance, and as the propagation distance increases, the beam with different beam widths at the source plane will have a similar beam spot in the far field,

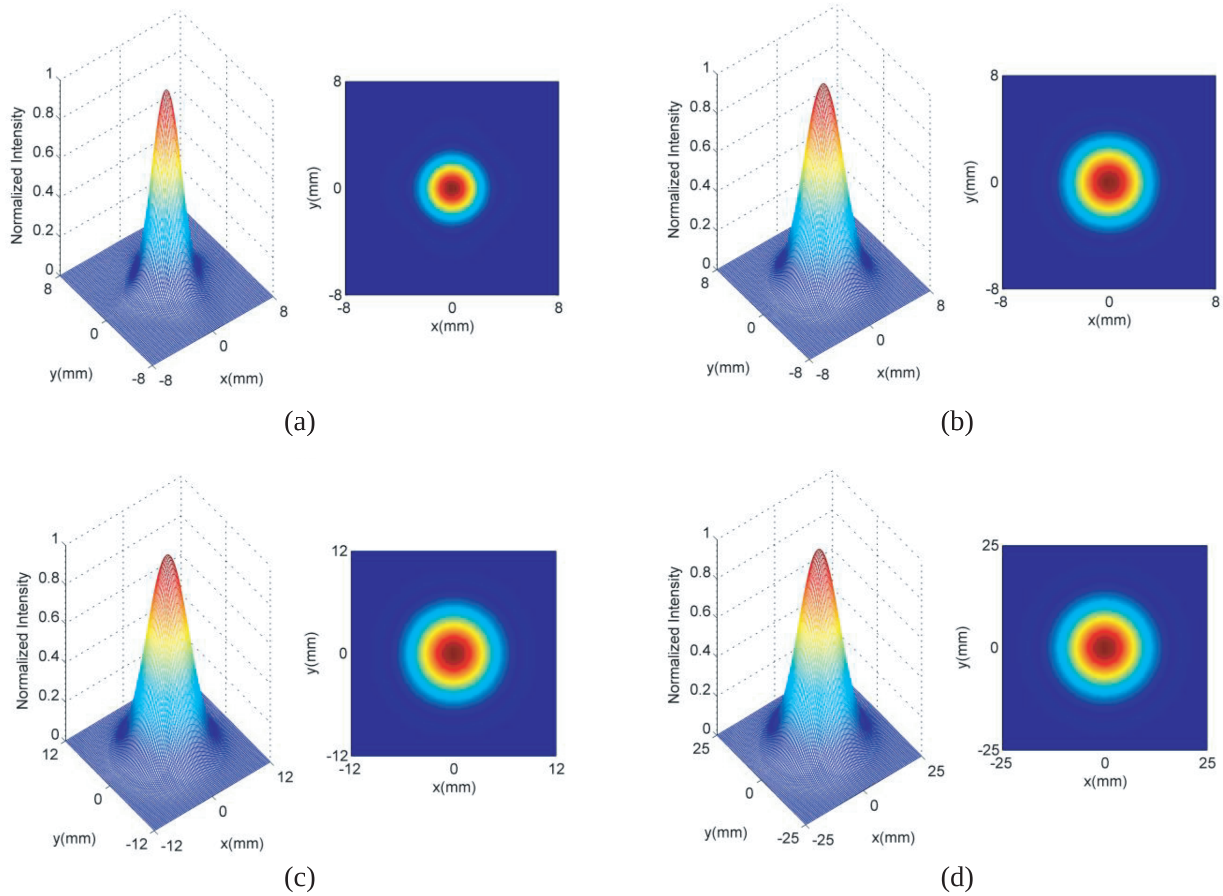

Figure 1. Normalized average intensity of the partially coherent Lorentz beam with $w_{0y} = 2\,\mathrm{mm}$ propagating in oceanic turbulence. (a) $z = 15\,\mathrm{m}$, (b) $z = 30\,\mathrm{m}$, (c) $z = 60\,\mathrm{m}$, (d) $z = 120\,\mathrm{m}$.

which can be explained as the partially coherent Lorentz beams with smaller width will have larger speed of spreading as the propagation distance increases.

Second, the influences of coherence length $\sigma_y = \sigma_y = \sigma$ on the average intensity of partially coherent Lorentz beams are given in Figure 4. It can be found that the partially coherent Lorentz beams with smaller coherence length will spread faster as the propagation distance z increases. The average intensity of fully coherent Lorentz beam ($\sigma = \inf$) is also given in Figure 4, and it can be found that the Lorentz beam will spread slower than partially coherent Lorentz beam when the beam propagates in oceanic turbulence.

At last, the influences of oceanic turbulence on the average intensity of partially coherent Lorentz beams propagating in oceanic turbulence are given in Figures 5–7. Form Figure 5, it can be seen that the partially coherent Lorentz beam in oceanic turbulence with smaller ε will evolve into Gaussian-like beam faster. When parameter ε of oceanic turbulence is smaller, the strength of oceanic turbulence is stronger. Figure 6 shows the influence of the relative strength of temperature and salinity fluctuations ς of oceanic turbulence on the average intensity of partially coherent Lorentz beams. One finds that the partially coherent Lorentz beam in oceanic turbulence with larger ς will evolve into Gaussian-like beam faster. When parameter ς is larger, the salinity of ocean water affects the strength of oceanic turbulence more than temperature of ocean water, and in this situation, the strength of oceanic turbulence will become stronger. From Figure 7, it is found that the partially coherent Lorentz beam in oceanic turbulence with larger x_T of oceanic turbulence will evolve into Gaussian-like beam faster than the beam with smaller x_T, and in this situation, the strength of oceanic turbulence is stronger.

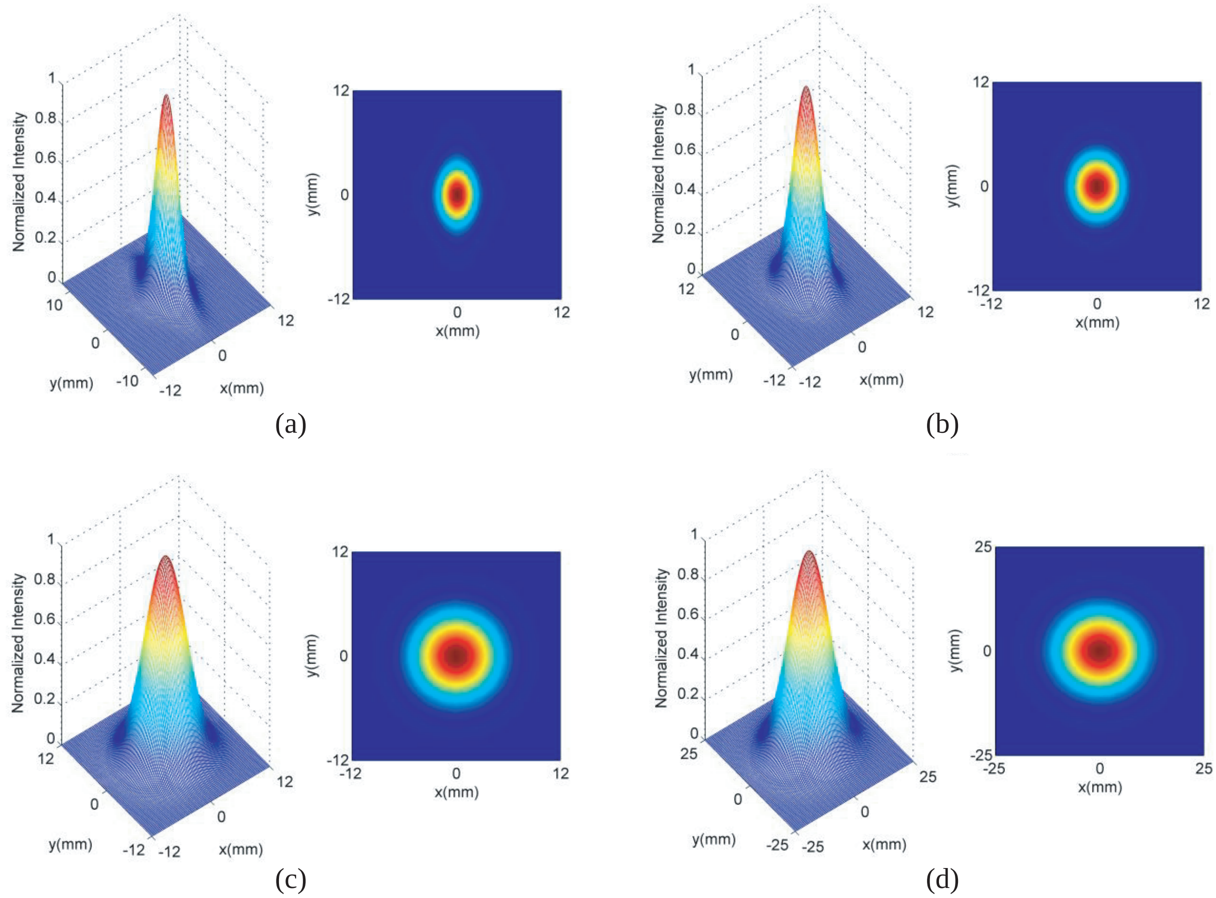

Figure 2. Normalized average intensity of the partially coherent Lorentz beam with $w_{0y} = 4\,\mathrm{mm}$ propagating in oceanic turbulence. (a) $z = 15\,\mathrm{m}$, (b) $z = 30\,\mathrm{m}$, (c) $z = 60\,\mathrm{m}$, (d) $z = 120\,\mathrm{m}$.

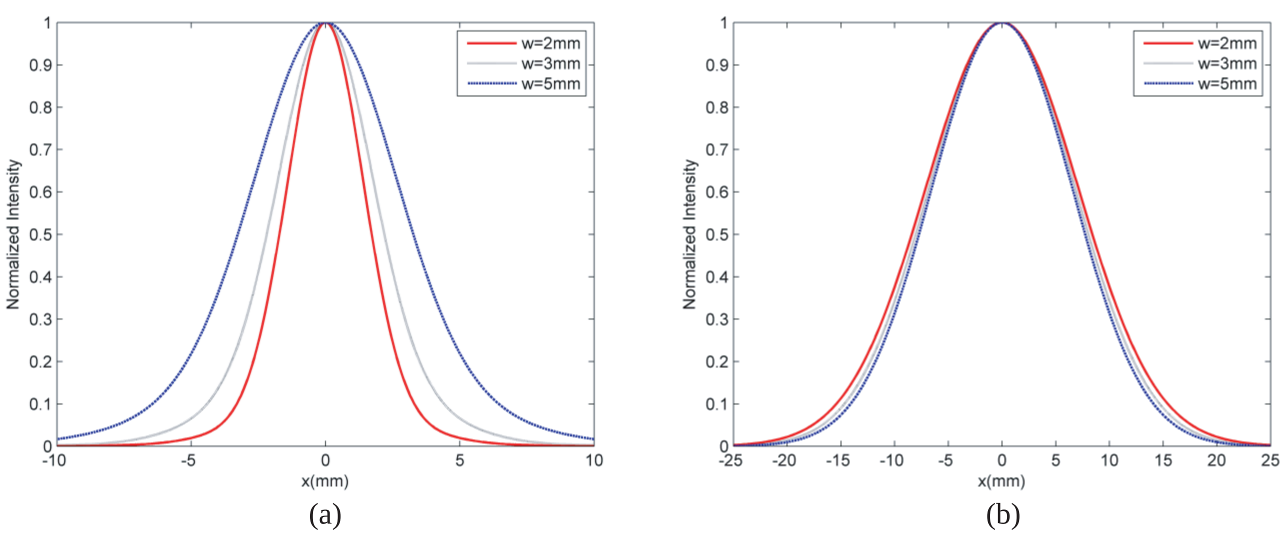

Figure 3. Cross sections ($y = 0$) of the partially coherent Lorentz beam propagating in oceanic turbulence for the different w. (a) $z = 15\,\mathrm{m}$, (b) $z = 120\,\mathrm{m}$.

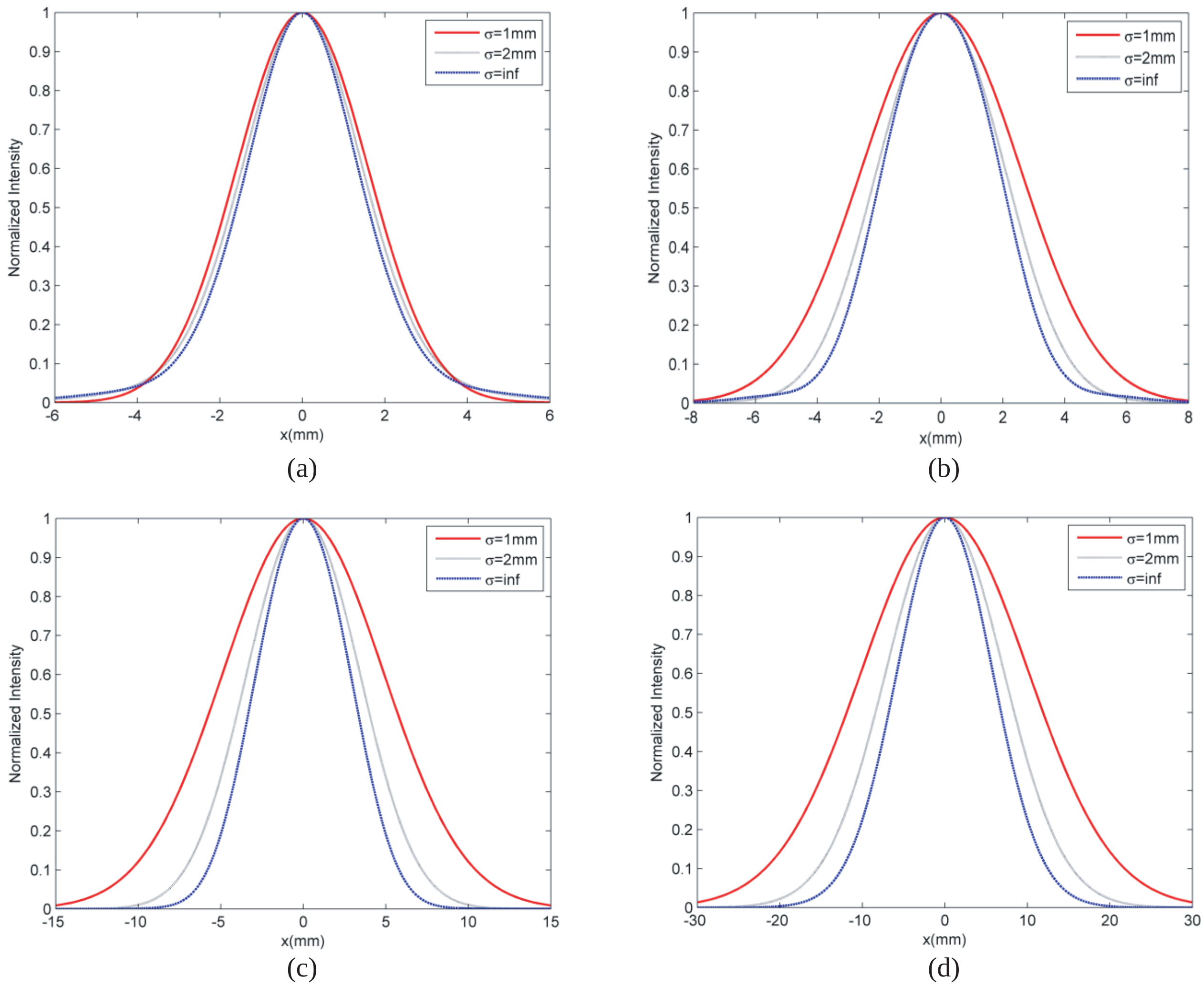

Figure 4. Cross sections ($y = 0$) of the partially coherent Lorentz beam propagating in oceanic turbulence for the different σ. (a) $z = 15\,\text{m}$, (b) $z = 30\,\text{m}$, (c) $z = 60\,\text{m}$, (d) $z = 120\,\text{m}$.

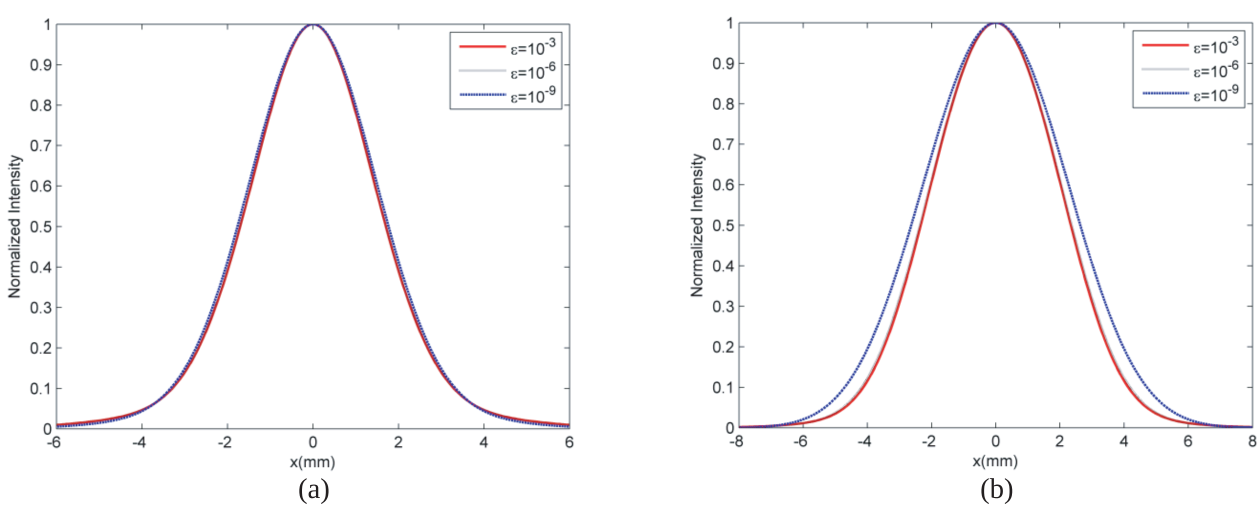

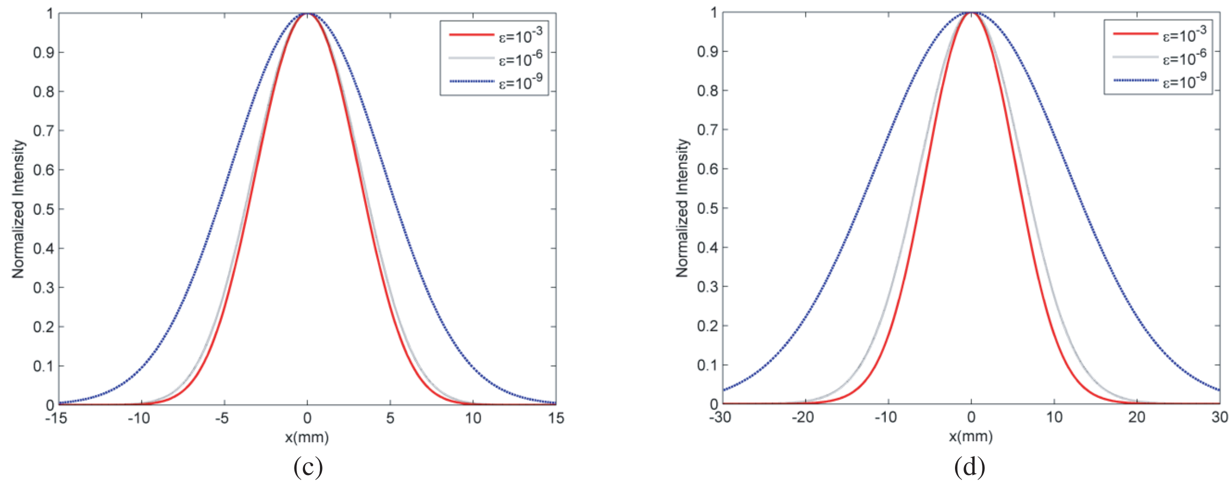

Figure 5. Cross sections ($y = 0$) of the partially coherent Lorentz beam propagating in oceanic turbulence for the different ε. (a) $z = 15\,\mathrm{m}$, (b) $z = 30\,\mathrm{m}$, (c) $z = 60\,\mathrm{m}$, (d) $z = 120\,\mathrm{m}$.

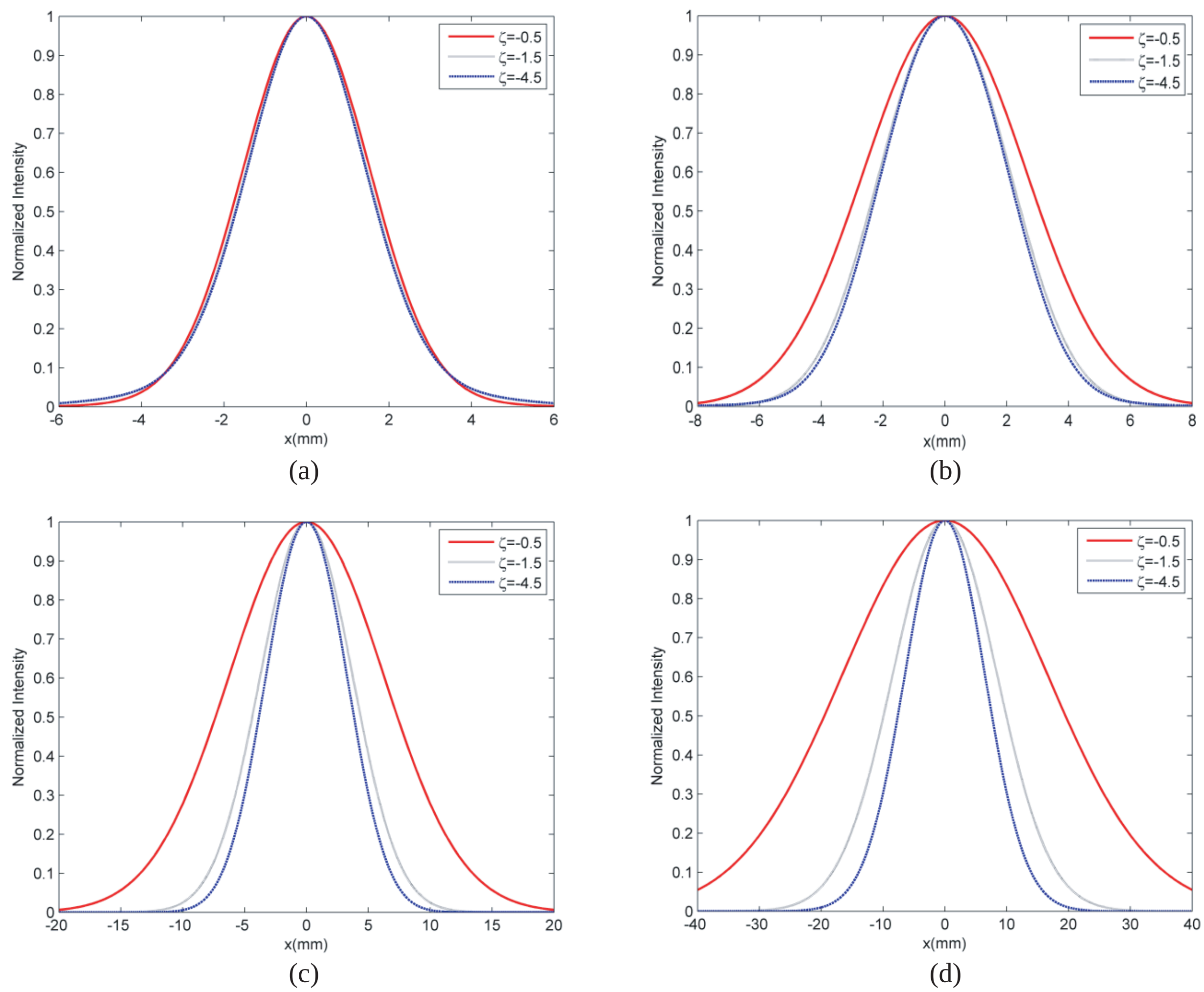

Figure 6. Cross sections ($y = 0$) of the partially coherent Lorentz beam propagating in oceanic turbulence for the different ς. (a) $z = 15\,\mathrm{m}$, (b) $z = 30\,\mathrm{m}$, (c) $z = 60\,\mathrm{m}$, (d) $z = 120\,\mathrm{m}$.

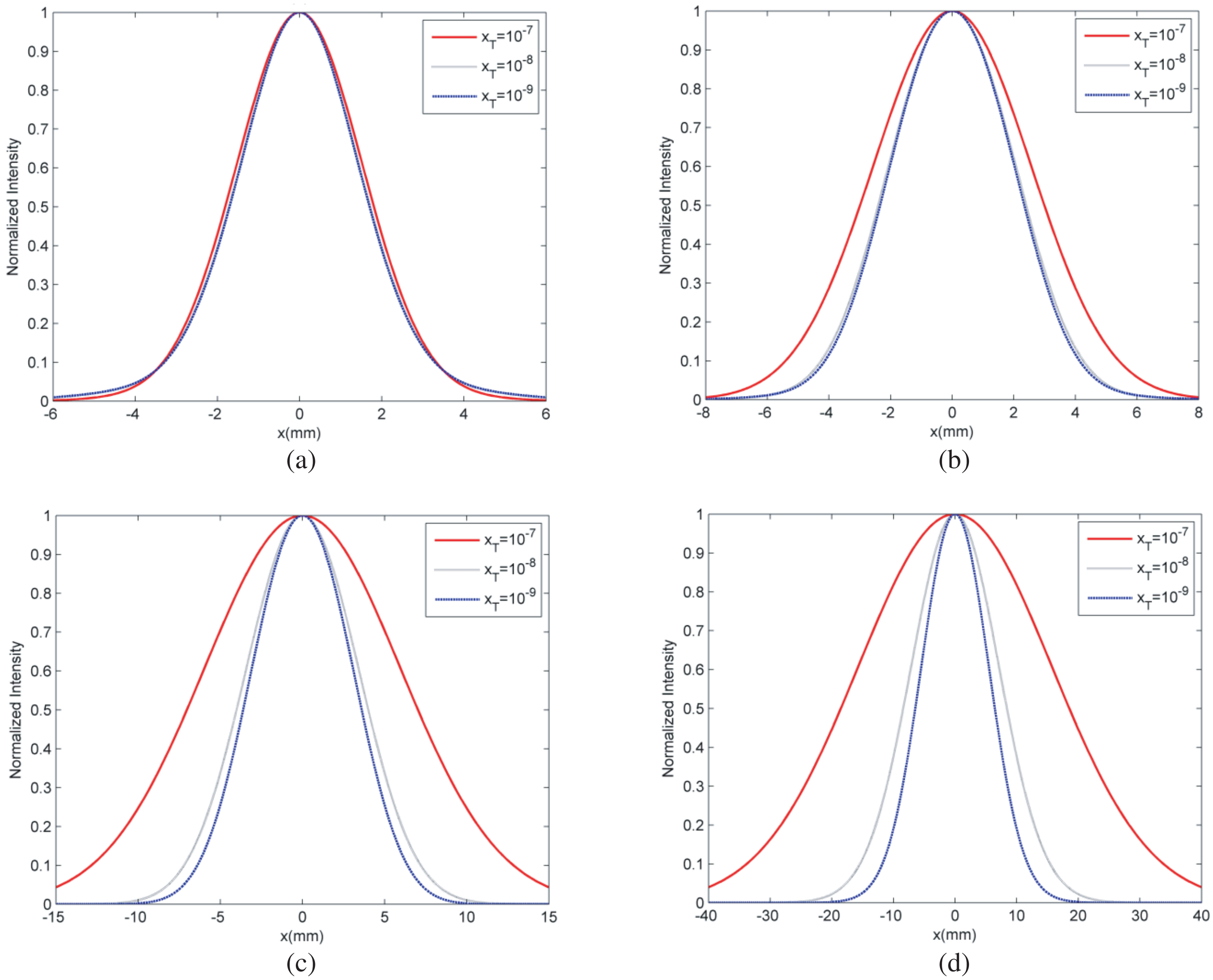

Figure 7. Cross sections ($y = 0$) of the partially coherent Lorentz beam propagating in oceanic turbulence for the different χ_T. (a) $z = 15\,\mathrm{m}$, (b) $z = 30\,\mathrm{m}$, (c) $z = 60\,\mathrm{m}$, (d) $z = 120\,\mathrm{m}$.

4. CONCLUSIONS

In this paper, based on the extended Huygens-Fresnel integral, the analytical propagation equations of partially coherent Lorentz beams in oceanic turbulence are derived. Using the derived equations, the average intensity of the partially coherent Lorentz beams in oceanic turbulence is analyzed and discussed using the numerical examples in detail. It is found that the partially coherent Lorentz beams propagating in oceanic turbulence will evolve into a Gaussian-like beam as the propagation distance increases, and the beam with smaller coherence length will spread faster. The beam propagation in stronger oceanic turbulence will spread rapidly as the propagation distance increases.

ACKNOWLEDGMENT

This work was supported by the National Natural Science Foundation of China (11604038, 11404048), Natural Science Foundation of Liaoning Province (201602062, 201602061) and the Fundamental Research Funds for the Central Universities (3132018235, 3132018236).

REFERENCES

1. El Gawhary, O. and S. Severini, "Lorentz beams and symmetry properties in paraxial optics," *Journal of Optics A: Pure and Applied Optics*, Vol. 8, 409–414, 2006.
2. Zhao, C. and Y. Cai, "Paraxial propagation of Lorentz and Lorentz-Gauss beams in uniaxial crystals orthogonal to the optical axis," *J. Mod. Optics*, Vol. 57, 375–384, 2010.
3. Ni, Y. Z. and G. Q. Zhou, "Nonparaxial propagation of Lorentz-Gauss vortex beams in uniaxial crystals orthogonal to the optical axis," *Appl. Phys. B: Lasers O*, Vol. 108, 883–890, 2012.
4. Zhou, G. Q., "Characteristics of paraxial propagation of a super Lorentz-Gauss SLG(01) mode in uniaxial crystal orthogonal to the optical axis," *Chinese Phys. B*, Vol. 21, 054104, 2012.
5. Liu, D., H. Yin, G. Wang, and Y. Wang, "Propagation properties of a partially coherent Lorentz beam in uniaxial crystal orthogonal to the optical axis," *Journal of the Optical Society of America A*, Vol. 34, 953–960, 2017.
6. Zhou, G. Q., "Propagation of a partially coherent Lorentz-Gauss beam through a paraxial ABCD optical system," *Opt. Express*, Vol. 18, 4637–4643, 2010.
7. Zhou, G., "Average intensity and spreading of super Lorentz-Gauss modes in turbulent atmosphere," *Appl. Phys. B: Lasers O*, Vol. 101, 371–379, 2010.
8. Zhou, G. and X. Chu, "M(2)-factor of a partially coherent Lorentz-Gauss beam in a turbulent atmosphere," *Appl. Phys. B: Lasers O*, Vol. 100, 909–915, 2010.
9. Zhou, P., X. Wang, Y. Ma, H. Ma, X. Xu, and Z. Liu, "Average intensity and spreading of a Lorentz beam propagating in a turbulent atmosphere," *J. Opt.-Uk*, Vol. 12, 015409, 2010.
10. Zhou, G. Q., "Propagation of a radial phased-locked Lorentz beam array in turbulent atmosphere," *Opt. Express*, Vol. 19, 24699–24711, 2011.
11. Zhao, C. L. and Y. J. Cai, "Propagation of partially coherent Lorentz and Lorentz-Gauss beams through a paraxial ABCD optical system in a turbulent atmosphere," *J. Mod. Optics*, Vol. 58, 810–818, 2011.
12. Liu, D., H. Yin, G. Wang, and Y. Wang, "Propagation of partially coherent Lorentz-Gauss vortex beam through oceanic turbulence," *Appl. Optics*, Vol. 56, 8785–8792, 2017.
13. Liu, D., G. Wang, and Y. Wang, "Average intensity and coherence properties of a partially coherent Lorentz-Gauss beam propagating through oceanic turbulence," *Optics & Laser Technology*, Vol. 98, 309–317, 2018.
14. Liu, D., Y. Wang, G. Wang, and H. Yin, "Influences of oceanic turbulence on Lorentz Gaussian beam," *Optik — International Journal for Light and Electron Optics*, Vol. 154, 738–747, 2018.
15. Zhou, G. Q., "Nonparaxial propagation of a super-Lorentz-Gauss SLG(01) mode beam," *Chinese Phys. B*, Vol. 19, 2010.
16. Zhou, G., "Propagation of vectorial Lorentz beam beyond the paraxial approximation," *J. Mod. Optics*, Vol. 55, 3573–3579, 2008.
17. Yu, H., L. L. Xiong, and B. D. Lu, "Nonparaxial Lorentz and Lorentz-Gauss beams," *Optik*, Vol. 121, 1455–1461, 2010.
18. Baykal, Y., "Scintillation index in strong oceanic turbulence," *Opt. Commun.*, Vol. 375, 15–18, 2016.
19. Baykal, Y., "Fourth-order mutual coherence function in oceanic turbulence," *Appl. Optics*, Vol. 55, 2976–2979, 2016.
20. Zhou, Y., Q. Chen, and D. M. Zhao, "Propagation of astigmatic stochastic electromagnetic beams in oceanic turbulence," *Appl. Phys. B: Lasers O*, Vol. 114, 475–482, 2014.
21. Liu, D. J., Y. C. Wang, and H. M. Yin, "Evolution properties of partially coherent flat-topped vortex hollow beam in oceanic turbulence," *Appl. Optics*, Vol. 54, 10510–10516, 2015.
22. Yang, T., X. L. Ji, and X. Q. Li, "Propagation characteristics of partially coherent decentred annular beams propagating through oceanic turbulence," *Acta Phys. Sin.-Ch. Ed.*, Vol. 64, 204206, 2015.

23. Huang, Y. P., B. Zhang, Z. H. Gao, G. P. Zhao, and Z. C. Duan, "Evolution behavior of Gaussian Schell-model vortex beams propagating through oceanic turbulence," *Opt. Express*, Vol. 22, 17723–17734, 2014.
24. Xu, J. and D. M. Zhao, "Propagation of a stochastic electromagnetic vortex beam in the oceanic turbulence," *Opt. Laser Technol.*, Vol. 57, 189–193, 2014.
25. Liu, D. J., L. Chen, Y. C. Wang, G. Q. Wang, and H. M. Yin, "Average intensity properties of flat-topped vortex hollow beam propagating through oceanic turbulence," *Optik*, Vol. 127, 6961–6969, 2016.
26. Huang, Y. P., P. Huang, F. H. Wang, G. P. Zhao, and A. P. Zeng, "The influence of oceanic turbulence on the beam quality parameters of partially coherent Hermite-Gaussian linear array beams," *Opt. Commun.*, Vol. 336, 146–152, 2015.
27. Liu, D., Y. Wang, G. Wang, X. Luo, and H. Yin, "Propagation properties of partially coherent four-petal Gaussian vortex beams in oceanic turbulence," *Laser Phys.*, Vol. 27, 016001, 2017.
28. Lu, L., Z. Q. Wang, J. H. Zhang, P. F. Zhang, C. H. Qiao, C. Y. Fan, and X. L. Ji, "Average intensity of $M \times N$ Gaussian array beams in oceanic turbulence," *Appl. Optics*, Vol. 54, 7500–7507, 2015.
29. Tang, M. M. and D. M. Zhao, "Regions of spreading of Gaussian array beams propagating through oceanic turbulence," *Appl. Optics*, Vol. 54, 3407–3411, 2015.
30. Lu, L., P. F. Zhang, C. Y. Fan, and C. H. Qiao, "Influence of oceanic turbulence on propagation of a radial Gaussian beam array," *Opt. Express*, Vol. 23, 2827–2836, 2015.
31. Dong, Y. M., L. N. Guo, C. H. Liang, F. Wang, and Y. J. Cai, "Statistical properties of a partially coherent cylindrical vector beam in oceanic turbulence," *J. Opt. Soc. Am. A*, Vol. 32, 894–901, 2015.
32. Liu, D. J., Y. C. Wang, G. Q. Wang, H. M. Yin, and J. R. Wang, "The influence of oceanic turbulence on the spectral properties of chirped Gaussian pulsed beam," *Opt. Laser Technol.*, Vol. 82, 76–81, 2016.
33. Liu, D. J. and Y. C. Wang, "Average intensity of a Lorentz beam in oceanic turbulence," *Optik — International Journal for Light and Electron Optics*, Vol. 144, 76–85, 2017.
34. Liu, D., Y. Wang, X. Luo, G. Wang, and H. Yin, "Evolution properties of partially coherent four-petal Gaussian beams in oceanic turbulence," *J. Mod. Optics*, Vol. 64, 1579–1587, 2017.
35. Schmidt, P., "A method for the convolution of lineshapes which involve the Lorentz distribution," *Journal of Physics B*, Vol. 9, 2331–2339, 1976.
36. Jeffrey, H. D. A., *Handbook of Mathematical Formulas and Integrals*, 4th edition, Academic Press Inc., 2008.